



Encapsulation and surface charge manipulation of organic and inorganic colloidal substrates by multilayered polyelectrolyte films



T. Mendoza-Dorantes^a, U. Pal^a, J.R. Vega-Acosta^b, C. Márquez-Beltrán^{a,*}

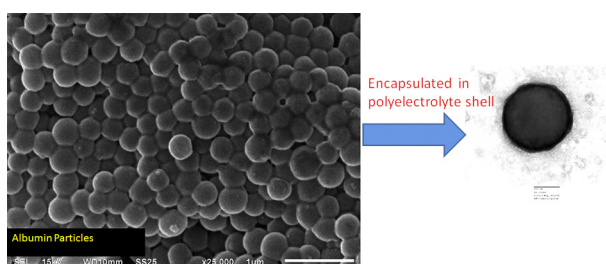
^a Instituto de Física, Benemérita Universidad Autónoma de Puebla, Apdo. Postal J-48 Puebla, Puebla 72570, Mexico

^b Instituto de Física, Universidad Autónoma de San Luis Potosí, San Luis Potosí 78290, Mexico

HIGHLIGHTS

- Bovine serum albumin protein nanoparticles were synthesized by coacervation process.
- BSA and SiO₂ particles could be encapsulated by multilayered polyelectrolyte films.
- Higher ζ -potential of BSA helps to keep the polyelectrolyte chains unfolded.
- Smooth capsulation layers could be formed over BSA nanoparticles.
- Nature of polyelectrolyte determines the nature of surface charge and ζ -potential.

GRAPHICAL ABSTRACT



ARTICLE INFO

Article history:

Received 1 March 2013

Received in revised form 3 May 2013

Accepted 7 May 2013

Available online 20 May 2013

Keywords:

Multilayer polyelectrolyte

ζ -Potential

Protein nanoparticle

ABSTRACT

Employing layer-by-layer (LbL) technique we could encapsulate both organic and inorganic nano- and microparticulate substrates by multilayer polyelectrolyte films of variable thicknesses. It has been observed that the uniformity of the polyelectrolyte multilayer does not depend severely on the chemical nature of particulate substrate; rather it depends on the initial surface charge density or ζ -potential of their bare surface. Higher ζ -potential of organic albumin nanoparticles helps to keep the polyelectrolyte chains unfolded. On the other hand, a lower ζ -potential of inorganic microparticles such as SiO₂ induces a folding of dangling polyelectrolyte chains, forming domains of their aggregates or complexes at the particle surface, making the encapsulating multilayer inhomogeneous.

© 2013 Elsevier B.V. All rights reserved.

1. Introduction

Encapsulation process has been traditionally exploited in the preparation of micro- and nano-capsules containing biologically active agents such as drugs, foods, and nutrients. Depending on the preparation process, those nanostructures can be classified as nanospheres and nanocapsules. While a spherical polymeric nanostructure with drug impregnated at its surface is called nanosphere

the particle containing drug at its interior is called nanocapsule [1,2]. For therapeutic applications, those polymeric nano- or microcapsules must be biodegradable [3]. During the past decade, several bio-polyelectrolytes, such as polysaccharides, polypeptides or polynucleotides, which are highly biodegradable both in vitro and in vivo, have been utilized for the fabrication of capsules [4]. However, after reaching at target sites, the nanocapsules need to release their encapsulated drugs in controlled fashion. Among the variety of drug releasing processes, those with remote functionalities, e.g. by external stimulations such as light [5–12], ultrasound [13], and magnetic field [14] are very much interesting for controlled drug release after administration. Another innovative way to achieve this goal in pharmacology can be by designing polymer

* Corresponding author. Fax: +52 222 2295611.

E-mail addresses: cmarquez@ifuap.buap.mx, cesmarbel2004@hotmail.com (C. Márquez-Beltrán).

nanoparticles with enhanced oral bioavailability containing peptides and proteins, as about 90% of all the nutrients, electrolytes, and water get absorbed in the small intestinal region of the gastrointestinal tract [15,16]. The entrapment of active molecules within polymeric nanoparticle would offer the protection of drug molecules against in vivo degradation by the surrounding environment after oral administration, and their undesired release [17].

The layer-by-layer (LbL) technique implemented by Decher [18] was initially applied for the construction of multilayered polyelectrolytes over flat substrates. The technique is based on the electrostatic attraction of oppositely charged polyelectrolytes adsorbed on solid surfaces. Adsorption of polyelectrolyte over a solid surface depends strongly on the cooperative interaction between the particle and the polyelectrolyte, apart from the influence of ionic strength of the solution, pH of the solution, and the porosity of the solid surface (substrate) [19–22]. These parameters can give rise to many forces such as steric, solvation, and hydrophobic, which control the behavior of end product. Later, the method LbL has been utilized to encapsulate solid or liquid colloidal substrates. Several colloidal substrates, such as melamine formaldehyde particles [23], SiO₂ microparticles [24–26], and carbonate microparticles such as MnCO₃, CdCO₃, and CaCO₃ [27,28] could be encapsulated using this technique. Most of these encapsulations were made under moderate temperature and pH values, without using any solvent that may cause damage to the encapsulating substrates. The method is advantageous for the fabrication of multilayer charged polyelectrolyte films, the thickness of which can be controlled just by the variation of number of formed layers. Controlling the thickness of encapsulating layer is very much important for drug delivery through polymer capsules.

The versatility of the LbL method has also allowed the production of hollow microcapsules by dissolving inorganic colloidal substrates in acids such as hydrochloric acid (HCl), tetrahydrofuran (THF), hydrogen fluoride (HF), and ethylene diamine tetracetic acid (EDTA) [28]. Apart from thickness, the permeability of these microcapsules depends on the structure and molecular weight of the constituting polymer(s). Their internal cavities could be loaded with different drug molecules such as biomedicine [29,30], DNA [31], and proteins [32,33] for different applications. To facilitate the release of those drug molecules from microcapsules, the thickness of the capsule walls should be less than 10 nm, which can only be achieved through LbL technique. Dong et al. [34] have shown that the capsule structure is dominated by two critical factors: the wall thickness, and the core decomposition condition. At optimized core removal conditions, capsule permeability has seen to be strongly dependent on wall thickness, which could be controlled by the variation of solvent quality (i.e. salt concentration) or the number of bilayers. The critical multilayer thickness for capsule preparation was about 10 nm.

On the other hand, interest for synthesizing protein nanoparticles (PNPs) has increased many folds in recent years due to their important functionalities in biomedicines such as good biocompatibility and integrity with ultrathin polyelectrolyte microreservoir templates. Using pectin as a pharmaceutical additive for the suppression of albumin nanoparticle agglomeration, they could be used as drug delivery systems, specially for antitumoral drugs, antibiotics, and gene delivery vehicles [33,35,36]. Different methods have been utilized to synthesize PNPs. The most popular among them are coacervation [35–37], and emulsion [36,38,39]. Coacervation is the mostly used method producing stable protein nanoparticle of controlled size in the 100–200 nm range. It is believed that protein nanoparticle have higher intercellular reception than micrometric particles [40] due to their higher specific surfaces (surface to mass ratios). While the colloidal stability of PNPs with high specific surface is a big concern for their practical applications, due to nanometric size they have the ability to cross

biological barriers. On the other hand, due to higher surface area, they make better and efficient contacts with living cells, facilitating a rapid release of delivered drug.

Among the common proteins, albumin is the one which contains in high concentration in human blood, synthesized in liver from dietary protein. Its presence in blood plasma creates an osmotic force that maintains fluid volume level in the vascular space. Though albumin has a short half-life, low albumin in blood is a sign of poor health and a predictor of a bad outcome. Application of albumin in medicine is mainly due to its surface functional groups such as thiol, amino- and carboxylic, which can form bonds with cell membrane. Due to the selective bonding nature of these functional groups, albumin gets accumulated at albumin arthritic and tumor sites [41,42], and hence used as a targeted drug delivery agent for releasing specific drugs, e.g. antitumor drugs.

While encapsulating inorganic particles such as SiO₂ with suitable semipermeable functional polymer is important for producing nanocapsules, functionalization of the surface of organic particles such as albumin with suitable bio-polyelectrolyte is necessary for their targeted delivery in living body. In this regard, though several efforts have been made to cover inorganic and organic nano- or microparticles by multilayered polyelectrolytes [27–29], controlling the thickness, surface charge and final shape of the particles, which depend both on the nature of substrate particle and the used polymer, had never been easy.

In the present article, we tried to fabricate polyelectrolyte multilayer films of alternating charges over silica and albumin particles by LbL technique to tailor their surface charge of desired polarity. Effects of multilayer polyelectrolyte encapsulation of the micro-/nanoparticles on their morphology and surface charge density have been studied.

2. Experimental

2.1. Materials

Albumin from bovine serum (BSA), sodium polystyrenesulfonate (PSS, $M_w \sim 7.0 \times 10^4$ g/mol), polyallylamine hydrochloride (PAH, $M_w \sim 5.6 \times 10^4$ g/mol), glutaraldehyde (8% solution) and Tween 20 were purchased from Sigma–Aldrich. All the chemicals were utilized as received without further purification. PSS and PAH solutions were prepared using deionized water (18 mΩ).

2.2. Fabrication of albumin nanoparticles

The albumin nanoparticles (ANPs) were prepared by a coacervation method based on the precipitation of albumin from its homogeneous solution by the addition of a non-solvent, followed by their chemical stabilization. For this purpose, we used an aqueous solution of BSA at 2 wt% (pH 9) and ethanol as desolvating agent, keeping the ethanol/water ratio 4:1. The nanoparticles were obtained through drop-wise addition of non-solvent (ethanol) and the addition of 100 μl of 8 wt% glutaraldehyde (GA) solution once the solution became turbid. Addition of GA induces a cross linking of the free amine groups, which helps to stabilize the ANPs. The reaction was performed at room temperature (24 °C) under magnetic stirring for 3 h. After this time, the ANPs were washed three times by centrifugation at 10,000 rpm for 20 min using deionized water.

2.3. Polymer encapsulation of ANPs and SiO₂ microparticles

The albumin and SiO₂ particles were encapsulated by polyelectrolyte multilayers using the LbL method. For the case of ANP encapsulation, the polyelectrolyte solutions were prepared at pH 7.0 maintaining the concentration of PAH, PSS and salt (NaCl) at 1.0 mM, 0.5 mM, and 0.1 M, respectively. Initially 1.0 mL of PAH

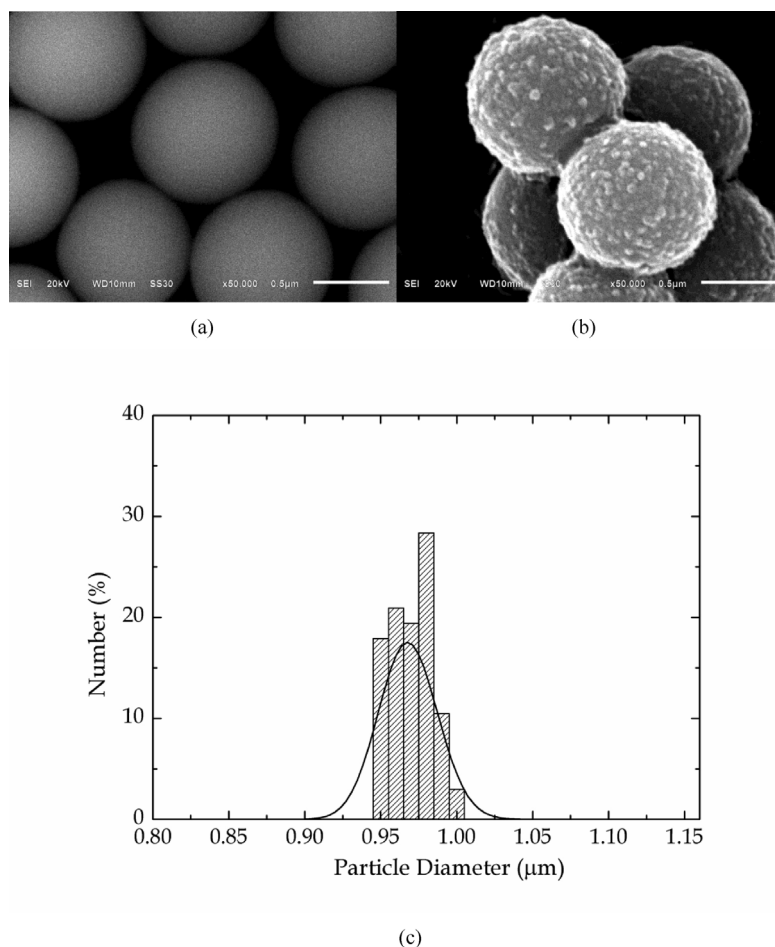


Fig. 1. Typical SEM images of (a) bare, (b) 3 PAH-PSS bilayer-capped silica particles, and (c) size distribution histogram of bare silica particles and its log-normal fitting. Roughening of the particle surface on bilayer formation is clear from the micrographs.

solution was added drop-wise (200 $\mu\text{L}/\text{min}$) to an aqueous suspension of ANP (0.01 wt%) under magnetic agitation. This mixture was left unagitated for another 10 min. After this time, the ANP-PAH were separated by centrifugation at 10,000 rpm and washed by deionized water three times. On achieving the PAH adsorption over ANPs, the PSS solution was added. After a 10 min aging time, the particles were separated and washed following the same procedure mentioned earlier. Once the PAH-PSS bilayer is formed over the ANPs, the LbL procedure was repeated to obtain six PAH-PSS bilayers. Similar procedure was followed to encapsulate SiO_2 microparticles in aqueous suspension with 0.1 wt%; nevertheless in this case we used 10 mM and 5.0 mM concentrations of PAH and PSS solutions, respectively.

2.4. Characterization of the micro- and nanoparticles

The morphology of the polymer coated and uncoated particles was studied in a JEOL JSM-6610LV scanning electron microscope (SEM) with a pre-centered W hairpin filament, operating at 15 kV. The samples for SEM study were prepared by dispersing the colloidal samples over silicon substrate (2 mm \times 2 mm) and drying in air.

2.5. Transmission electron microscopy (TEM)

Aliquots of the samples were dispersed over copper microgrids, whose surfaces were made hydrophilic by glow discharge process,

and dried at room temperature. After that, the samples were stained with 1% uranyl acetate for 30 s and dried with filter paper. A JEOL JEM-1230 transmission electron microscope operating at 80 kV was utilized to inspect the samples.

2.6. ζ -Potential

The ζ -potential values of the polyelectrolyte coated and uncoated ANPs and SiO_2 particles were measured in a MALVERN-ZEN 3600 Zetasizer. Electrophoretic mobility of each sample was measured at least five times dispersing them in deionized water. The essence of a classical micro-electrophoresis system is a cell with electrodes at either end to which a potential is applied. Particles move toward the electrode of opposite charge, and their velocity is measured. This velocity expressed per unit field strength is considered as its electrophoretic mobility of the particles. With this knowledge we can estimate the ζ -potential of the particles using the Henry equation:

$$U_E = \frac{2\varepsilon\zeta f(ka)}{3\eta}, \quad (1)$$

where U_E is the electrophoretic mobility, ε and η are the dielectric constant and viscosity of the dispersion medium, respectively, and $f(ka)$ the Henry's function, which involves Debye length (k) and radius (a) of the colloidal particles.

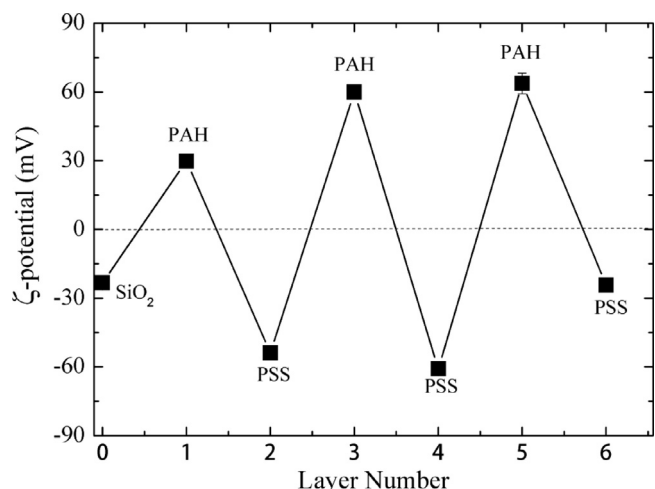


Fig. 2. Variation of ζ -potential of the silica surface with the number of alternating PAH and PSS capping layers. Alternate variation of surface charge suggests a stepwise growth of multilayers.

3. Results and discussion

Fig. 1 shows the typical SEM images of SiO₂ particles before and after the assembly of three PAH–PSS bilayers. As can be seen in Fig. 1a, the bare SiO₂ particles are well dispersed, of uniform size with smooth surfaces. Average diameter of the particles estimated from their size distribution histogram (Fig. 1c) was about $0.968 \pm 0.036 \mu\text{m}$. On covering the microparticles with PAH–PSS bilayers (Fig. 1b), their surfaces become rough. The observed morphology change suggests the polyelectrolytes adsorbed on SiO₂ surface form domains.

Despite of vast experimental works performed using LbL technique, the details of multilayer formation is not fully understood, specially for a charged colloidal sphere. The formation of polyelectrolyte domains over the SiO₂ microparticles in the present case is probably due to a significant gain in entropy of the floating polyelectrolyte chains away from the substrate surface. The polyelectrolyte chains away from the substrate surface have greater degrees of freedom with respect to the chains near (or attached to) the substrate surface, generating a cooperative interaction between the closer and far ends (with respect to the substrate), which leads to the formation of polymer aggregates or polyelectrolyte complex on the substrate surface. Through their theoretical studies, Messina et al. [43] have demonstrated the role of short range van der Waals like attraction between the surface charge of spherical substrates and the oppositely charged adsorbed polymer chains. They found in particular that below a certain value of the strength of the specific van der Waals attraction, formation of globular polymer structures is highly favorable, whereas for higher van der Waals attraction, a flat bilayer builds up. Therefore, the morphology of polymer layers over solid substrates depends on the interaction between the polymer and the substrate surface. On forming four PAH–PSS bilayers over the microparticles of SiO₂, we obtained polyelectrolyte layers of about 50 nm average thickness, indicating the thickness of each bilayer of about 12.5 nm.

ζ -Potential of the SiO₂ microparticles was estimated after the formation of each bilayer. Variation of ζ -potential of the silica surface with the increase of layer number in the process of PAH–PSS bilayer formation is shown in Fig. 2. It must be noted that the bilayers over the silica particles were formed at pH 7 of the reaction solution. As can be observed, the ζ -potential of the silica surface alternates between positive and negative values on adding each layer of polyelectrolyte. As it could be expected, the nature of the final surface charge is determined by the nature of the formed

Table 1

Variation of adsorbed PSS concentration over the surface of SiO₂ microparticles with the number of formed PAH–PSS bilayers.

No. of PAH–PSS bilayers	Absorbance at 225 nm	PSS adsorbed concentration (mM)
1	0.681	0.0216
2	0.2186	0.0281
3	0.3821	0.0491
4	0.4432	0.0569

bilayer. In the present case, the surface ζ -potential of the particles covered with a fixed number of PAH–PSS bilayer would be negative. The ζ -potential value for the bare SiO₂ particles was about -23.28 mV . On the formation of first polyelectrolyte (PAH) layer, the ζ -potential of their surface changes the sign to positive, confirming the adsorption/attachment of PAH layer over the silica surface. In our encapsulation process, the odd layer numbers are associated with the formation of PAH layers and even layer numbers are associated with the formation of PSS layers over the SiO₂ particles. As can be seen, all the ζ -potential values for the surfaces terminated by PAH (odd layer numbers) layer are positive, varying in between $+58$ and $+70 \text{ mV}$. On the other hand, all the ζ -potential values for the surfaces terminated by PSS (even layer numbers) are negative, varying in between -55 and -66 mV .

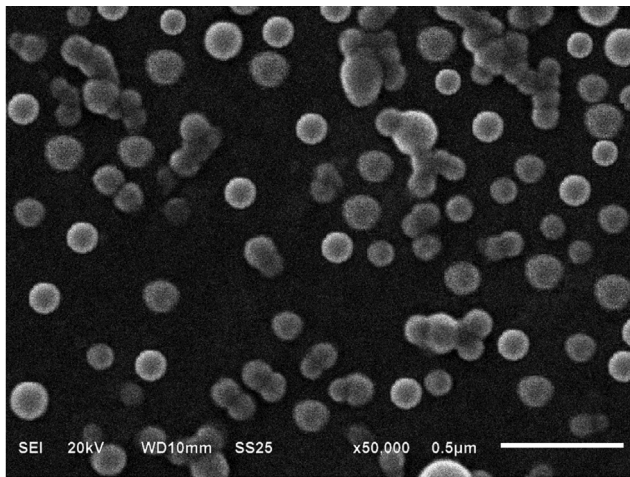
The concentration of polyelectrolyte adsorbed at SiO₂ surface was determined from their optical absorption spectra in the 200–400 nm range, utilizing a Cary-500 UV-Vis spectrophotometer, and comparing the absorbance with the calibrated absorbance of PSS solution of different concentrations. The estimated concentrations of adsorbed PSS after the formation of each PAH–PSS bilayer are presented in Table 1. As can be seen, on increasing the number of bilayers, the concentration of adsorbed PSS increases linearly at the rate of $1.27 \times 10^{-2} \text{ mM/PAH–PSS bilayer}$. Considering the molecular weight of used PSS ($\sim 7 \times 10^4 \text{ g/mol}$), amount of used SiO₂ particles (0.1 wt%) and their average diameter ($0.968 \mu\text{m}$) the amount of PSS adsorbed in each bilayer over each silica particle was calculated to be about $1.12 \times 10^{-5} \mu\text{g}$.

The results obtained so far indicate that the LbL method is a useful technique for encapsulating inorganic colloidal particles. On encapsulating the silica microparticles with four PAH–PSS bilayers, their surface become rough due to the formation of polyelectrolyte domains, and a maximum 0.0569 mM concentration of PSS could be adsorbed, which is about 1.13% of the concentration of PSS in its initial solution (5.0 mM).

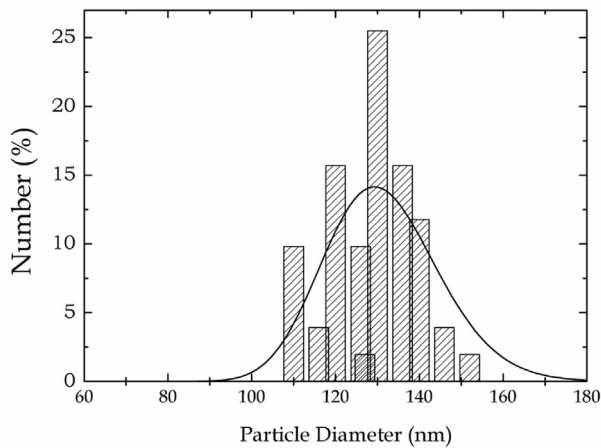
4. Albumin encapsulation

As has been mentioned in Section 2, the ANPs were synthesized by coacervation method, utilizing ethanol as a non-solvent followed by crosslinking with glutaraldehyde. The SEM image of the bare ANPs (Fig. 3a) reveals the formation of well dispersed spherical particles with average diameter of about $131 \pm 15 \text{ nm}$ (Fig. 3b). Addition of glutaraldehyde in the coacervation process reduces the aggregation of albumin molecules desolvated with ethanol. GA form cross-links with the ANPs forming covalent bond between its aldehyde (CHO) groups and the terminal amino (NH₂) groups of cysteine protein (albumin) [44,45]. The formation of cross-links provides stability to the albumin particles by decreasing the protein–protein aggregation and thus preventing their precipitation. As the main aim of this article is to study the encapsulation of SiO₂ and albumin particles by LbL process and control of their surface charge, we will not discuss on either the coacervation process or on the stability of ANPs in details.

Typical TEM images of ANPs encapsulated with four polyelectrolyte layers (two PAH–PSS bilayers) are shown in Fig. 4. As can be



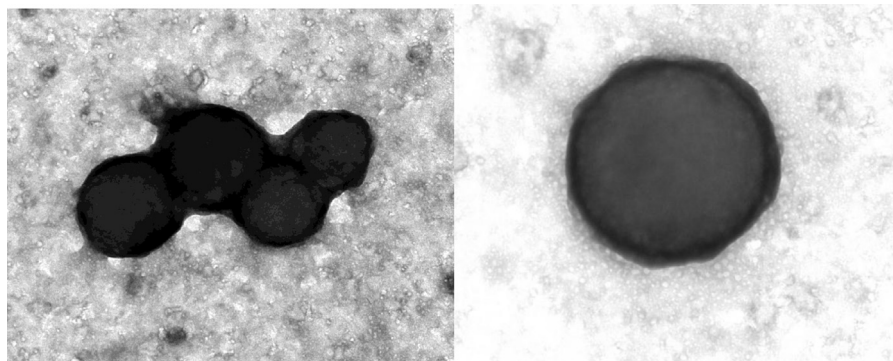
(a)



(b)

Fig. 3. (a) Typical SEM image of bare BSA nanoparticles obtained via coacervation process and (b) their size distribution histogram with log-normal fitting.

seen, the polymer-capped ANPs get agglomerated easily. Formation of polyelectrolyte layer over the particles is very clear from the TEM image presented in Fig. 4b. The image shows a clear contrast difference between the internal and external parts of the encapsulated



(a)

(b)

Fig. 4. Typical TEM images of albumin particles covered with 4 polyelectrolyte layers (2 PAH-PSS bilayers). (a) Agglomeration of nanocore-shell structures with darker polyelectrolyte shell layers and (b) single submicron core-shell structure.

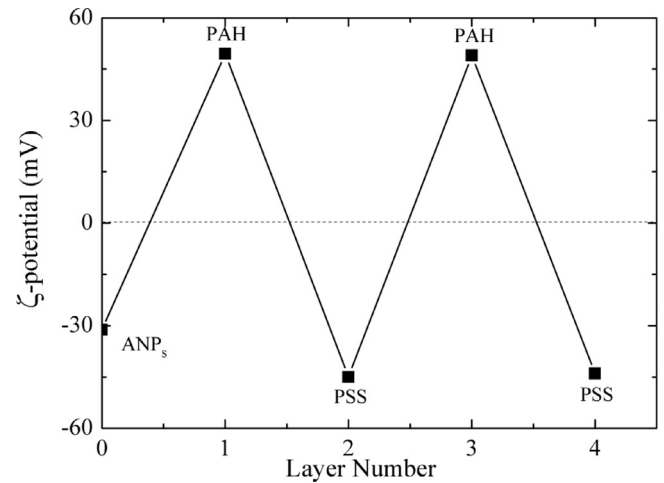


Fig. 5. Variation of the ζ -potential value of ANPs with the number of formed polyelectrolyte layers. Charge inversion in very regular manner with the number of capping layers indicates the formation of uniform polyelectrolyte layers.

particle, confirming the adsorption of polyelectrolyte at the surface of ANPs and the formation of uniform shell layer. It must be noted that in case of SiO_2 microparticles, the polyelectrolyte shell was irregular due to the formation of domains at particle surface.

ζ -Potential values of the multilayers formed on the ANPs are shown in Fig. 5. The variation of ζ -potential value with the number of polyelectrolyte layers (PAH and PSS alternatively) was very similar to the case of SiO_2 , with a charge reversal on the formation of each adsorbed layer. However, in this case, the ζ -potential value for the bare ANPs revealed to be more negative (-31.22 mV) in comparison with SiO_2 microparticles. Addition of first polyelectrolyte layer (PAH layer) induced positive charge at the surface of ANPs. On the other hand, the next polyelectrolyte layer (PSS layer) induced a negative charge at their surface. In the fashion similar to the earlier case (SiO_2 microparticles), every odd numbered capping layer (correspond to PAH) revealed positive ζ -potential values varying in between $+49.5$ and $+49$ mV, and every even numbered layer (correspond to PSS) revealed negative ζ -potential values varying in between -45 and -44 mV. The magnitudes of ζ -potential of the first and second bilayers were similar, which indicates the formation of uniform multilayers at the surface of ANPs. Apart from the differences of surface nature between the two types of studied particles, it seems the smaller sizes of the ANPs are favorable for

the formation of uniform polyelectrolyte layers over them. It must be noticed that the ζ -potential value for the naked ANPs is stronger than the ζ -potential value of the naked SiO₂ NPs.

The ζ -potential is related to the charge density and morphology (flat or roughness) of the adsorbed polyelectrolyte layer(s) on particle surface. In the case of protein nanoparticles, a constant charge density suggests the formation of uniform polyelectrolyte layer. However, in the case of silica particle, the multilayers were not uniform due to the formation of polyelectrolyte aggregates at their surfaces, and hence the surface charge density was not constant. These findings show how the nature of substrate (inorganic and organic) surface affects the formation of multilayer capping or the charge distribution over them.

5. Conclusion

We have demonstrated that the LbL method can be effectively used to encapsulate both inorganic and organic particles of micrometer or nanometer size by polyelectrolyte multilayer to control the nature of their surface charge. The thickness, and hence indirectly the permeability of the encapsulation layer can be controlled by controlling the number of formed polyelectrolyte layers. The synthesis of protein nanoparticles by coacervation method is a versatile and easy way for fabricating nanoparticles of sizes below 170 nm. The use of glutaraldehyde as cross linking agent helps to prevent aggregation of nanoparticles in solution, obtaining well dispersed nanoparticles with uniform size distribution. As the nanoparticle uptake by most of the cells of human organisms is restricted to 50–200 nm size range, the encapsulated protein nanoparticle presented in this work could be useful for cellular therapy. Furthermore, the protein nanoparticles obtained in this work and their encapsulation via the self-assembly of oppositely charged polyelectrolytes optimize the method of fabrication of polymer capsules containing protein molecules.

Acknowledgements

The work was financially supported by VIEP, BUAP (VIEP/EXC/2012-27) and CONACyT (Grant # CB-2010/151767), Mexico. The authors are thankful to Dr. Efraín Rubio Rosas for his help in taking SEM micrographs of the samples. The Zetasizer facility extended by UASLP, Mexico is also acknowledged.

References

- [1] M.J. Alonso, Nanomedicines for overcoming biological barriers, *Biomed. Pharmacother.* 58 (2004) 168–172.
- [2] P. Couvreur, G. Barratt, E. Fattal, P. Legrand, C. Vauthier, Nanocapsule technology: a review, *Crit. Rev. Ther. Drug Carrier Syst.* 19 (2002) 99–134.
- [3] Bruno G. De Geest, Stefaan De Koker, Gleb B. Sukhorukov, Oliver Kreft, Wolfgang J. Parak, Andrei G. Skirtach, Jo Demeester, Stefaan C. De Smed, Wim E. Hennink, Polyelectrolyte microcapsules for biomedical applications, *Soft Matter* 5 (2009) 282–291.
- [4] C. Picart, A. Schneider, O. Etienne, J. Mutterer, P. Schaaf, C. Egles, N. Jessel, J.C. Voegel, Controlled degradability of polysaccharide multilayer films in vitro and in vivo, *Adv. Funct. Mater.* 15 (2005) 1771–1780.
- [5] B.G. De Geest, N.N. Sanders, G.B. Sukhorukov, J. Demeester, S.C. De Smedt, Release mechanisms for polyelectrolyte capsules, *Chem. Soc. Rev.* 36 (2007) 636–649.
- [6] A.S. Angelatos, B. Radt, F. Caruso, Light-responsive polyelectrolyte/gold nanoparticle microcapsules, *J. Phys. Chem. B* 109 (2005) 3071–3076.
- [7] B. Radt, T.A. Smith, F. Caruso, Optically addressable nanostructured capsules, *Adv. Mater.* 16 (2004) 2184–2189.
- [8] A.G. Skirtach, A.A. Antipov, D.G. Shchukin, G.B. Sukhorukov, Remote activation of capsules containing Ag nanoparticles and IR dye by laser light, *Langmuir* 20 (2004) 6988–6992.
- [9] A.G. Skirtach, C. Dejugnat, D. Braun, A.S. Susa, A.L. Rogach, W.J. Parak, H. Mohwald, G.B. Sukhorukov, The role of metal nanoparticles in remote release of encapsulated materials, *Nano Lett.* 5 (2005) 1371–1377.
- [10] A.G. Skirtach, A. Munoz Javier, O. Kreft, K. Köhler, A. Alberola Piera, H. Mohwald, W.J. Parak, G.B. Sukhorukov, Laser-induced release of encapsulated materials inside living cells, *Angew. Chem. Int. Ed.* 45 (2006) 4612–4617.
- [11] X. Tao, J.B. Li, H. Mohwald, Self-assembly, optical behavior, and permeability of a novel capsule based on an azo dye and polyelectrolytes, *Chem. Eur. J.* 10 (2004) 3397–3403.
- [12] B.G. De Geest, A.G. Skirtach, T.R.M. De Beer, G.B. Sukhorukov, L. Bracke, W.R.G. Baeyens, J. Demeester, S.C. De Smedt, Stimuli-responsive multilayered hybrid nanoparticle/polyelectrolyte capsules, *Macromol. Rapid Commun.* 28 (2007) 88–95.
- [13] D.G. Shchukin, D.A. Gorin, H. Mohwald, Ultrasonically induced opening of polyelectrolyte microcontainers, *Langmuir* 22 (2006) 7400–7404.
- [14] Z.H. Lu, M.D. Prouty, Z.H. Guo, V.O. Golub, C. Kumar, Y.M. Lvov, Magnetic switch of permeability for polyelectrolyte microcapsules embedded with Co@Au nanoparticles, *Langmuir* 21 (2005) 2042–2050.
- [15] P.V. Balimane, S. Chong, Cell culture-based models for intestinal permeability: a critique, *Drug Discov. Today* 10 (2005) 335–343.
- [16] K.J. Lee, N. Johnson, J. Castelo, P.J. Sinko, G. Grass, K. Holme, Y.H. Lee, Effect of experimental pH on the in vitro permeability in intact rabbit intestine and caco-2 monolayer, *Eur. J. Pharm. Sci.* 25 (2005) 193–200.
- [17] B. Mashkevich (Ed.), *Drug Delivery Research Advances*, Nova Science Pub. Inc., New York, 2007, pp. 39–76 (Chapter 2).
- [18] G. Decher, Fuzzy nanoassemblies toward layered polymeric multicomposites, *Science* 277 (1997) 1232–1237.
- [19] G.B. Sukhorukov, A.A. Atipov, A. Voigt, H. Mohwald, pH-controlled macromolecule encapsulation in and release from polyelectrolyte multilayer nanocapsules, *Macromol. Rapid. Commun.* 22 (2001) 44–46.
- [20] F.N. Crespihlo, V. Zucolotto, O.N. Oliveira Jr., F.C. Nart, Electrochemistry of layer-by-layer films: a review, *Int. J. Electrochem. Sci.* 1 (2006) 194–214.
- [21] V. Milkova, T. Radeva, The effect of ionic strength on electrical properties of polyelectrolyte multilayers on colloidal particles, *J. Phys. Condens. Matter* 22 (2010), 494107 (6pp).
- [22] A.A. Antipov, G.B. Sukhorukov, Polyelectrolyte multilayer capsules as vehicles with tunable permeability, *Adv. Colloid Interface Sci.* 111 (2004) 49–61.
- [23] G.B. Sukhorukov, E. Donath, H. Lichtenfeld, E. Knippel, M. Knippel, A. Budde, H. Möhwald, Layer-by-layer self assembly of polyelectrolytes on colloidal particles, *Colloid Surf. A* 137 (1998) 253–266.
- [24] R.N. Smith, M. McCormick, C.J. Barrett, L. Reven, H.W. Spiess, NMR studies of PAH/PSS polyelectrolyte multilayers adsorbed onto silica, *Macromolecules* 37 (2004) 4830–4838.
- [25] J.H. Wosnick, J.H. Liao, T.M. Swager, Layer-by-layer poly(phenylene ethynylene) films on silica microspheres for enhanced sensory amplification, *Macromolecules* 38 (2005) 9287–9290.
- [26] S.C. Peyratout, L. Dhane, Tailor-made polyelectrolyte microcapsules: from multilayers to smart containers, *Angew. Chem. Int. Ed.* 43 (2004) 3762–3783.
- [27] G.B. Sukhorukov, D.V. Volodkin, A.M. Gunther, A.I. Petrov, D.B. Shenoy, H. Mohwald, Porous calcium carbonate microparticles as templates for encapsulation of bioactive compounds, *J. Mater. Chem.* 14 (2004) 2073–2081.
- [28] M.L. De Temmerman, J. Demeester, F. De Vos, S.C. De Smedt, Encapsulation performance of layer-by-layer microcapsules for proteins, *Biomacromolecules* 12 (2011) 1283–1289.
- [29] H. Ai, J.J. Pink, X. Shuai, D.A. Boothman, J. Gao, Interactions between self-assembled polyelectrolyte shells and tumor cells, *Inc. J. Biomed. Mater. Res.* 73 (2005) 303–312.
- [30] J.S. Temoff, H. Park, E. Jabbari, D.E. Conway, T.L. Shffield, C.G. Ambrose, A.G. Mikos, Thermally cross-linked oligo(poly(ethylene glycol) fumarate) hydrogels support osteogenic differentiation of encapsulated marrow stromal cells in vitro, *Biomacromolecules* 5 (2004) 5–10.
- [31] D.G. Shchukin, A.A. Patel, G.B. Sukhorukov, Y.M. Lvov, Nanoassembly of biodegradable microcapsules for DNA encasing, *J. Am. Chem. Soc.* 126 (2004) 3374–3375.
- [32] A.I. Petrov, D.V. Volodkin, G.B. Sukhorukov, Protein–calcium carbonate coprecipitation: a tool for protein encapsulation, *Biotechnol. Prog.* 21 (2005) 918–925.
- [33] G.K. Gupta, V. Jain, P.R. Mishra, Templated ultrathin polyelectrolyte microreservoir for delivery of bovine serum albumin: fabrication and performance evaluation, *Pharm. Sci. Tech.* 12 (2011) 344–353.
- [34] W.F. Dong, J.K. Ferri, T. Adalsteinsson, M. Schöhoff, G.B. Sukhorukov, H. Möhwald, Influence of shell structure on stability, integrity, and mesh size of polyelectrolyte capsules: mechanism and strategy for improved preparation, *Chem. Mater.* 17 (2005) 2603–2611.
- [35] P.V. Kumar, N.K. Jain, Suppression of agglomeration of ciprofloxacin-loaded human serum albumin nanoparticles, *Pharm. Sci. Tech.* 8 (2007) E118–E123.
- [36] M. Rahimnejad, Z. Babaei, Protein nanoparticle: a unique system as drug delivery vehicles, *J. Biotechnol.* 7 (2008) 4926–4934.
- [37] W. Lin, A.G.A. Coombes, M.C. Davies, L. Illum, Preparation of sub-100 nm human serum albumin nanospheres using a pH-coacervation method, *J. Drug Target.* 1 (1993) 237–243.
- [38] U. Scheffel, B. Rhodes, T.K. Natarajan, H.N. Wagner, Albumin microspheres for study of the reticuloendothelial system, *J. Nucl. Med.* 13 (1972) 498–503.
- [39] B.G. Muller, H. Leuenberger, T. Kissel, Albumin nanospheres as carriers for passive drug targeting: an optimized manufacturing technique, *Pharm. Res.* 13 (1996) 32–37.
- [40] J. Panyam, V. Labhasetwar, Biodegradable nanoparticles for drug and gene delivery to cells and tissue, *Adv. Drug Deliv. Rev.* 55 (2003) 329–347.

- [41] Y. Takakura, T. Fujita, M. Hashida, H. Sezaki, Disposition characteristics of macromolecules in tumor-bearing mice, *J. Pharm. Res.* 7 (1990) 339–346.
- [42] F. Kratz, Albumin as a drug carrier: design of prodrugs, drug conjugates and nanoparticles, *J. Control. Release* 132 (2008) 171–183.
- [43] R. Messina, C. Holm, K. Kremer, Polyelectrolyte multilayering on a charged sphere, *Langmuir* 19 (2003) 4473–4482.
- [44] J.A. Kiernan, Formaldehyde, formalin, paraformaldehyde and glutaraldehyde: What they are and what they do, *Microsc. Today* 1 (2000) 8–12.
- [45] I. Migneault, C. Dariguenave, M.J. Bertrand, K.C. Waldron, Glutaraldehyde: behavior in aqueous solution, reaction with proteins, and application to enzyme crosslinking, *Bio Techniques* 37 (2004) 790–802.